DMD Fast Forward. Published on February 15, 2012 as doi:10.1124/dmd.111.042291
This article has not been copyedited and formatted. The final version may differ from this version.

DMD #42291

TARGET-MEDIATED PHARMACOKINETIC AND PHARMACODYNAMIC MODEL OF EXENDIN-4 IN RATS, MONKEYS AND MAN

WEI GAO AND WILLIAM J. JUSKO

Department of Pharmaceutical Sciences, School of Pharmacy and Pharmaceutical Sciences, University of Buffalo, Buffalo, NY 14260

Running Title: PK/PD modeling of Exendin-4 in rats, monkeys and man

Corresponding author: William J. Jusko, 565 Hochstetter Hall, Department of Pharmaceutical Sciences, University at Buffalo, State University of New York. Buffalo, New York 14260

Phone: 716-645-2855

Fax: 716-645-3693

Email: wjjusko@buffalo.edu

Text pages: 20

Tables: 4

Figures: 8

References: 23

Words in Abstract: 249

Words in Introduction: 476

Words in Discussion: 1450

Abbreviations: TMDD: target-mediated drug disposition; PK: pharmacokinetics; PD: pharmacodynamics; GLP-1: glucagon-like peptide-1; GLP-1R: GLP-1 receptor.

DMD Fast Forward. Published on February 15, 2012 as DOI: 10.1124/dmd.111.042291
This article has not been copyedited and formatted. The final version may differ from this version.

ABSTRACT

A mechanism-based pharmacokinetic-pharmacodynamic (PK/PD) model was developed for exendin-4 to account for receptor-mediated endocytosis via GLP-1 receptor (GLP-1R) as the primary mechanism for its nonlinear disposition. Time profiles of exendin-4 concentrations following intravenous (iv), subcutaneous (sc) and continuous iv infusion doses in rats, iv and sc doses in monkeys, and iv infusion and sc doses in man were examined. Mean data for glucose and insulin after glucose challenges during exendin-4 treatment in healthy rats were analyzed. The PK model components included receptor binding, subsequent internalization and degradation, non-specific tissue distribution, and linear first-order elimination from plasma. The absorption rate constant (k_a) decreased with increasing doses in all three species. The clearance from central compartment (CL_c) (rats: 3.62 ml/min, monkeys: 2.39 ml/min/kg, man: 1.48 ml/min/kg) was similar to reported renal clearances. Selected PK parameters (CL_c, V_c and k_{off}) correlated allometrically with body weight. The equilibrium dissociation constant (K_D) was within the reported range in rats (0.74 nM), while the value in monkeys (0.12 pM) was much lower than in man (1.38 nM). The effects of exendin-4 on the glucose-insulin system were described by a feedback model with a biphasic effect equation driven by free exendin-4 concentrations. Our generalized nonlinear PK/PD model for exendin-4 taking into account of drug binding to GLP-1R well described PK profiles following various routes of administration over a large range of doses in three species along with PD responses in healthy rats. The present model closely reflects underlying mechanisms of disposition and dynamics of exendin-4.

INTRODUCTION

Exendin-4 is a 39 amino acid glucagon-like peptide-1 (GLP-1) analog, sharing approximately 53% sequence identity with mammalian GLP-1 (Doyle and Egan, 2007). Exendin-4 binds to pancreatic GLP-1 receptors (GLP-1R) to exhibit anti-diabetic actions, including glucose-dependent stimulation of insulin secretion, suppression of glucagon secretion, slowing of gastric emptying, satiety, and, in preclinical models, protection of beta-cells. In addition to the pancreas, GLP-1 receptors are also expressed in various tissues such as brain, lung and kidneys (Korner et al., 2007).

The disposition of exendin-4 in man has been reported as linear over the therapeutic dose range from 5 to 10 ug (Cvetkovic and Plosker, 2007). However, the pharmacokinetics (PK) of exendin-4 was reported as nonlinear in monkeys (Ai et al., 2008). In addition, the Bateman function could not describe the concentration-time profiles over certain ranges of doses in rats with one set of elimination parameter values (Gedulin et al., 2008), suggesting that the PK in rats may also be nonlinear. Furthermore, the simple Bateman function does not well represent the underlying mechanism of exendin-4 disposition, such as receptor binding and internalization. The major route of exendin-4 elimination was suggested to be glomerular filtration with subsequent enzyme degradation (Copley et al., 2006). But in rats with kidneys surgically removed, exendin-4 slowly disappeared from the system (Parkes, 2001), indicating the existence of non-renal clearance. As GLP-1R exist in various tissues and after binding to exendin-4, exendin-4-GLP-1R complexes are internalized and targeted for further degradation, we reasoned that receptor-mediated endocytosis and

degradation may be responsible for the non-renal clearance and the observed nonlinear behavior of exendin-4.

A general model for drugs exhibiting target-mediated drug disposition (TMDD) exists (Mager and Jusko, 2001). After administration, drug can be distributed to the peripheral compartment, directly eliminated, or bind to receptors. The drug-receptor complexes can be eliminated or dissociated to free receptors. The TMDD model uses receptor binding and receptor-mediated endocytosis as the primary mechanism of nonlinear drug disposition. Recently, we successfully captured the disposition of exendin-4 in diabetic rats using the TMDD model (Gao and Jusko, 2011). However, the PK of exendin-4 in other species has not been assessed using mechanistic modeling.

Generally, the in vivo pharmacological effects of exendin-4 have been evaluated either qualitatively or by comparing empirical measures such as the area under the plasma glucose and insulin concentration-time curves. Mechanism-based pharmacokinetic/pharmacodynamic (PK/PD) models can provide improved insights into drug actions. Mager et al characterized the effects of exendin-4 on glucose-insulin homeostasis under hyperglycemic clamping with a mechanism-based PD model, but used a hypothetical linear PK function (Mager et al., 2004).

We sought to carefully analyze exendin-4 disposition and effects using a mechanism-based PK/PD modeling approach in various species. This report characterizes the disposition of exendin-4 following doses of intravenous (iv), subcutaneous (sc) or iv infusion in rats, monkeys, and man using a TMDD PK/PD model to describe the insulintropic effects of exendin-4.

DMD Fast Forward. Published on February 15, 2012 as DOI: 10.1124/dmd.111.042291
This article has not been copyedited and formatted. The final version may differ from this version.

METHODS

The time profiles of exendin-4 concentrations in rats and man were obtained from studies conducted by Amylin Pharmaceuticals, Inc. The mean concentrations of exendin-4 in monkeys were captured by computer digitization from a publication (Ai et al., 2008). For the model fittings, all concentration data were converted to pmol/L units, and drug doses were converted to total moles using the molecular weight of exendin-4 of 4186.6.

In the rat PK study, male Sprague-Dawley (SD) rats (body weight 350-370 g, n = 4-7) received exendin-4 via three different routes - iv, continuous iv infusion, and sc bolus - at three doses: 0.5, 5, and 50 nmol (bolus injection), and at 0.5, 5, and 50 nmol/hr (iv infusion). Samples were assayed using a two-site sandwich assay developed at Amylin Pharmaceuticals, Inc. The minimum detectable concentration of exendin-4 was 15 pmol/L.

In another study, male SD rats (body weight 380-420 g, n = 4-8) were infused iv using the same volume of saline or exendin-4 at 3, 30, 300, and 3000 pmol/kg/min for 2 hours. At 30 min after beginning the infusion, D-glucose (5.7 mmol/kg) was injected iv at a rate of 0.5 ml/min over 2 to 3 min. Plasma glucose was determined by immobilized oxidase chemistry on an YSI 2300 Stat Plus, and insulin was determined by radioimmunoassay (Linco Research, St Charles, MO).

In the monkey PK study (Ai et al., 2008), male rhesus monkeys (body weight 4.3 ± 0.7 kg, n = 3) were given either a single sc injection of 1, 3, 10 μg/kg, or a single iv injection of 3 μg/kg. Serum exendin-4 concentrations were measured using a

DMD Fast Forward. Published on February 15, 2012 as DOI: 10.1124/dmd.111.042291
This article has not been copyedited and formatted. The final version may differ from this version.

radioimmunoassay. The linear range of this assay was 25-2000 pg/ml and the limit of quantitation of was 25 pg/mL.

Data from three human studies were included in the current analysis. In study A (Kolterman et al., 2005), 8 subjects (body weight 88.5 ± 9.4 kg) received 0.1, 0.2, 0.3, or 0.4 µg/kg sc doses of exendin-4. In study B (Kolterman et al., 2005), 8 subjects (body weight 88.8 ± 12.1 kg) received single sc doses of 0.02, 0.05 or 0.1 µg/kg. In study C (Degn et al., 2004), 11 subjects (BMI 21-29 kg/m^2) received an iv infusion of exendin-4 at 0.066 pmol/kg/min (0.276 ng/kg/min) for 360 min. Plasma exendin-4 concentrations were measured by Amylin Pharmaceuticals, Inc. (San Diego, CA) using an immunoenzymetric assay.

Pharmacokinetic model

For initial data evaluation, mean profiles of exendin-4 for each iv dose obtained from rats were used to perform a noncompartmental analysis (NCA) and curve fitting to a biexponential equation ($C = C_1 \cdot e^{-\lambda 1 \cdot t} + C_2 \cdot e^{-\lambda 2 \cdot t}$) using WinNonlin 5.0 (Pharsight Corp., NC) to evaluate dose-dependent changes in clearance (*CL*), steady-state volume of distribution (V_{ss}), and distributional clearance (CL_D).

For the next stage, a mechanism-based modeling approach was used for data analysis. The general scheme of the applied PK/PD model is presented in Figure 1. The free exendin-4 (*C*) in plasma can bind to GLP-1R (*R*) with a second-order rate constant (k_{on}) to form drug-receptor complex (*RC*), distribute to and from tissues (A_T) by first-order rates (k_{pt} and k_{tp}), and be directly eliminated (k_{el}). The RC can dissociate at a first-order rate (k_{off}) and be internalized and degraded (k_{int}). The GLP-1R (R) is assumed to remain constant (R_{tot}). The TMDD PK model can be described by:

DMD Fast Forward. Published on February 15, 2012 as DOI: 10.1124/dmd.111.042291
This article has not been copyedited and formatted. The final version may differ from this version.

$$\frac{dC}{dt} = input(t) - (k_{el} + k_{pt}) \cdot C + k_{tp} \cdot A_T / V_C - k_{on} \cdot R \cdot C + k_{off} \cdot RC; \qquad \text{Eq.1}$$
$$C(0) = Dose/V_C (iv) \, or \, 0 \, (sc, infusion.)$$

$$\frac{dA_T}{dt} = k_{pt} \cdot C \cdot V_C - k_{tp} \cdot A_T; \qquad A_T(0) = 0 \qquad \text{Eq. 2}$$

$$\frac{dRC}{dt} = k_{on} \cdot (R_{tot} - RC) \cdot C - (k_{off} + k_{int}) \cdot RC; \qquad RC(0) = 0 \qquad \text{Eq. 3}$$

where V_C represents the volume of the free exendin-4 (central) compartment.

The input function for Eq.1 following sc doses is:

$$input(t) = k_a \cdot F \cdot Dose \cdot exp(-k_a \cdot t) / V_C \qquad \text{Eq. 4}$$

where k_a is the first-order absorption rate constant and F is the absolute bioavailability after sc doses.

Pharmacodynamic model

The PD model proposed for insulintropic effects of exendin-4 is shown in Figure 1. The basic structure, the feedback model, represents the interregulated interaction between glucose and insulin: glucose (Glu) stimulates insulin secretion with a linear stimulation factor S_{Glu}, and insulin (Ins) stimulates glucose uptake with a linear stimulation factor S_{Ins}. The homeostasis of glucose and insulin were described by two indirect response models: k_{outG} and k_{outI} are the first-order output rate constants, and k_{inG} and k_{inI} are the zero-order input rate constants with the relationship of $k_{inG} = k_{outG} \cdot G_b$ and $k_{inI} = k_{outI} \cdot I_b$, where G_b and I_b are the basal glucose and insulin concentrations.

For initial evaluation, the simple feedback model was fitted to all the paired glucose and insulin profiles. All of the parameter estimates were comparable between dose groups, except for parameter S_{Glu}. The next step was to apply the feedback model

DMD Fast Forward. Published on February 15, 2012 as DOI: 10.1124/dmd.111.042291
This article has not been copyedited and formatted. The final version may differ from this version.

to glucose and insulin profiles for all rats, only allowing S_{Glu} to change among the dose groups.

For the next stage, a mechanism-based PKPD modeling approach was utilized for data analysis. Drug concentrations were simulated using the TMDD PK model and parameter values from the PK study. The PK driving function enhances glucose-dependent stimulation of insulin secretion by the biphasic Adair function (S_d). Equations for the feedback model for glucose and insulin concentrations are:

$$\frac{dGlu}{dt} = k_{inG} - k_{outG} \cdot (1 + S_{Ins} \cdot (Ins - I_b)) \cdot Glu; \qquad Glu(0) = Dose/V_G + G_b \qquad \text{Eq. 5}$$

$$\frac{dIns}{dt} = k_{inI} \cdot (1 + S_{Glu} \cdot (Glu - G_b) \cdot (1 + S_d)) - k_{outI} \cdot Ins; \qquad Ins(0) = I_b \qquad \text{Eq. 6}$$

$$S_d = \frac{S_{max} \cdot C}{k_1 + C + k_2 \cdot C^2} \qquad \text{Eq. 7}$$

where S_{max} is the maximum stimulation factor of the response; k_1 and k_2 are constants in the Adair function. The baseline condition G_b and I_b were fixed as the measured pre-dose values.

Using RC as the driving function for the effects of exendin-4 was also tested:

$$S_{d\ RC} = \frac{S_{max\,RC} \cdot RC}{k_{1\ RC} + RC + k_{2\ RC} \cdot RC^2} \qquad \text{Eq. 8}$$

All computer fittings and simulations were done using ADAPT II (BMSR, USC, CA) with the maximum likelihood method. The variance model was $V_i = (\sigma_1 + \sigma_2 \cdot Y)2$ where V_i is the variance of the ith data point, σ_1 and σ_2 are the variance model parameters, and Y_i represents the ith model predicted value.

DMD Fast Forward. Published on February 15, 2012 as DOI: 10.1124/dmd.111.042291
This article has not been copyedited and formatted. The final version may differ from this version.

RESULTS

Pharmacokinetics

The TMDD model has been used to capture the exendin-4 disposition in diabetic rats (Gao and Jusko, 2011) and adequately described exendin-4 PK in rats, monkeys and humans in this report. As shown in the model scheme (Figure 1), the TMDD model consists of target-binding (k_{on}, k_{off}), internalization and degradation of the receptor complex (k_{int}), non-specific tissue distribution (A_T), and a linear elimination pathway (k_{el}) from V_c.

Rat PK

The mean exendin-4 concentration-time profiles after various doses in rats are shown in Figure 2. The PK profiles show biexponential decline with typical characteristics of TMDD where low doses showed rapid decline in early times after iv injection and after stopping the iv infusion. Following iv injection, terminal half-lives ranged from 20 to 40 min with increasing doses. The NCA results from the mean profiles of exendin-4 are summarized in Table 1. Slope parameters λ_1, λ_2, and CL decreased with increasing exendin-4 doses. Generally, due to the limited target binding capacity, drugs exhibiting TMDD show saturable distribution, with a decrease in apparent distribution parameters (CL_D and V_{ss}) with increasing doses. However, this trend was observed in CL_D but not in V_{ss} for exendin-4 in rats. GLP-1Rs are widely expressed in non-pancreatic tissues, and these receptors may also contribute as binding sites for exendin-4, thus making changes in V_{ss} not evident. In addition, the apparent steady-state concentrations (C_{ss}) resulting from continuous infusion were not

DMD Fast Forward. Published on February 15, 2012 as DOI: 10.1124/dmd.111.042291
This article has not been copyedited and formatted. The final version may differ from this version.

dose-proportional. After sc injection, terminal half-lives were 120 to 200 min, indicating involvement of flip-flop kinetics.

In order to detect and properly quantify nonlinearities in PK, a wide range of drug doses is required. In man, disposition of exendin-4 has been described as linear over a narrow dose range, and the nonlinearity might also be hidden by flip-flop kinetics after sc injection. Straightforward evidence of nonlinear kinetics in rats was the lack of dose-proportionality of NCA parameters and C_{ss} resulting from continuous infusion (Table 1).

Early blood sampling is particularly important to capture binding characteristics of drugs with the general TMDD model and concentrations around the K_D value are desired. In the rat study, data were available from 5 min after iv bolus dosing and via various administration routes and observed concentrations ranged widely around the K_D value.

All parameters were estimated (Table 2) with reasonable precision (< 50% except for k_{off}). The clearance ($CL_c = k_{el} \cdot V_c$) is 3.62 ml/min, which is very close to the reported renal clearance (3.44 ml/min) (Parkes, 2001). The equilibrium dissociation constant K_D (= k_{off}/k_{on} = 0.74 nmol/L) is in the range of the reported values for specific binding of exendin-4 and GLP-1 to normal rat tissues (Goke et al., 1993; Goke et al., 1995; Larsen et al., 1997; Satoh et al., 2000). The total receptor concentrations (R_{tot}) was estimated to be 5.21 nmol/L for SD rats. The internalization rate constant was slightly higher than k_{el}. Bioavailability was estimated as close to 1 and then fixed as 1 in the final model. The absorption rate constant in rats decreased with increasing dose.

Monkey PK

DMD Fast Forward. Published on February 15, 2012 as DOI: 10.1124/dmd.111.042291
This article has not been copyedited and formatted. The final version may differ from this version.

The fitted profiles of exendin-4 in monkeys following various iv and sc doses are presented in Figure 3, and parameter estimates are listed in Table 3. The model well described monkey PK profiles, and yielded parameter estimates with reasonable CV%, except for parameters related to the drug-receptor complex (k_{on}, k_{off} and k_{int}). The value of CL_c was 2.39 ml/kg/min, within the range of GFR in healthy monkeys (2.2-3.6 ml/kg/min) (Altaian and Dittmer, 1974). The K_D value in monkeys was 0.12 pmol/L, which is 5000-fold lower than estimated in rats. The internalization rate constant in monkeys was 15 times lower than k_{el}. Bioavailability was around 70%, and the absorption rate constant decreased with dose, as observed in rats.

Man PK

The model-predicted time profiles of exendin-4 in three human studies are shown in Figure 4 and parameter estimates are listed in Table 3. The TMDD model adequately described the PK profiles from the three studies, but was unable to estimate total receptor content (R_{tot}), thus this parameter was fixed as a computer generalized value of 1.24 nmol/L. This value is 3.2 fold lower than the R_{tot} estimate in rats, which agrees with one observation where rat receptor density in lung and thyroid gland was as 2-5.5-fold of human receptor density (Korner et al., 2007). Since concentrations only after sc doses and one continuous iv infusion dose were available, it is no surprise that parameters were estimated with generally high CV%, especially for k_{on}, k_{off} and k_{int}. The CL_c was 1.48 ml/min/kg, almost identical to GFR in healthy subjects (125 ml/min in a 70 kg man). Bioavailability was fixed as 1 and the absorption rate constants were lower at higher doses as was also found in other species. A population modeling approach with more extensive data would improve these parameter estimates.

DMD Fast Forward. Published on February 15, 2012 as DOI: 10.1124/dmd.111.042291
This article has not been copyedited and formatted. The final version may differ from this version.

Pharmacodynamics

Increases of glucose and insulin after glucose challenge during continuous infusion of exendin-4 in rats are shown in Figure 5. Since no drug concentrations were measured in this study, the drug PK profiles (Figure 6A) were simulated according to the TMDD model and parameter values. Exendin-4 almost (>80%) reached steady-state after 30 min of infusion, at which time glucose was injected.

The next step was to evaluate the appropriateness of the feedback model describing the glucose and insulin physiological system in rats. The model reasonably characterized the glucose and insulin profiles, and all parameters, except for S_{Glu}, had similar values between control and other dose groups. Therefore, the feedback model well represents the glucose-insulin system in rats. The initial analysis also showed that drug treatment only affected S_{Glu}, the stimulation factor of glucose on insulin production, which was in agreement with the mechanism of action of exendin-4 on beta cells. Thus, in the next step of modeling, all rats shared the same set of parameters, but S_{Glu} was allowed to change. As shown in Figure 6B, the estimated S_{Glu} values first increased and then decreased with drug concentrations at the time of glucose challenge (C_{30min}). The Adair function (Adair, 1923) was able to characterize the bell-shaped relationship between S_{Glu} and C_{30min}, and Figure 6B depicts the fitted curve with this function.

The drug-receptor complex (*RC*) was also tested as the driving force for PD. The model fitted the concentration profiles well, but failed to generate precise parameters (ADAPT II was not able to provide CV% for parameter estimates). In addition, AIC values also favored *C* as the driving force. On the other hand, the PD study design did not contain enough information to differentiate the driving force of the PD effect, as both

C and *RC* reached apparent steady-states by the time of glucose injection. In addition, in a rat study conducted in our lab, maximum insulin stimulation occurred prior to maximum *RC*, indicating that the PD effect was better driven by *C (Gao and Jusko, 2011)*.

In the final PK/PD model, the plasma concentrations (*C*) were used to stimulate insulin release (Eq. 7). As shown in Figure 5, the present integrated PK/PD model adequately characterized glucose and insulin. Parameters controlling glucose and insulin metabolism were estimated with good precision (<80%) and comparable with literature values. The k_{out} values for glucose and insulin were 0.046 and 0.483 min^{-1}, corresponding to half-lives of 15 and 1.5 min. The estimated S_{max} was 4.67 and k_1 and k_2 were 0.826 nmol and 0.0153 $nmol^{-1}$.

DMD Fast Forward. Published on February 15, 2012 as DOI: 10.1124/dmd.111.042291
This article has not been copyedited and formatted. The final version may differ from this version.

DISCUSSION

Exendin-4, a potent GLP-1R agonist, exhibits insulintropic effects in a variety of animal models and man. This study, to our knowledge, is the first instance of applying a mechanistic model to quantify the disposition of exendin-4 in various species and the dynamics of exendin-4 in healthy rats. The general TMDD model delineating receptor-mediated drug disposition was proposed to characterize the nonlinear kinetic behavior across species. The likely mechanism of action was integrated into an existing model of the glucose-insulin system, thereby facilitating the simultaneous analysis of glucose and insulin responses to glucose challenge and drug effects.

Pharmacokinetics

The binding of exendin-4 to GLP-1R can be saturated at high ligand doses which contributes to the saturable clearance of exendin-4, although this has not been experimentally quantified. Recently, we reported that exendin-4 followed TMDD kinetics in Goto-Kakizaki (GK) diabetic rats (Gao and Jusko, 2011). Generally, the parameter estimates were similar between SD rats (in the current report) and GK rats. Comparisons of the two rat strains were discussed previously (Gao and Jusko, 2011).

The primary elimination route of exendin-4 has been proposed as glomerular filtration and k_{el} physiologically represents renal elimination (Copley et al., 2006). The linear CL_c in rats, monkeys and man was very close to reported renal clearances or GFR in healthy species. In rats, the relative contribution of CL_c to the total clearance was about 73% at the lowest dose, and nearly 100% at the highest doses. The V_c in the three species was larger than plasma (serum in monkeys) volume. Simple allometry was assessed for various parameters. Figure 7 shows the correlation between selected

DMD Fast Forward. Published on February 15, 2012 as DOI: 10.1124/dmd.111.042291
This article has not been copyedited and formatted. The final version may differ from this version.

PK parameters (CL_c, V_c, k_{off}) and body weights. The allometric exponents for CL_c and k_{off} are close to 0.75 and for V_c close to 1, similar to typical theoretical values. As was observed for type I interferon PK (Kagan et al., 2011), other PK parameters did not show a meaningful trend with body weight.

The GLP-1R undergoes endocytosis and, in the presence of agonist, the receptor cycles between the plasma membrane and endosomal compartment. The internalization of rat GLP-1R was examined in cell lines, with k_{on} as 0.082 L/min.nmol and k_{off} as 0.015 and 0.21 min^{-1} (Widmann et al., 1995). Our estimated k_{on} was about 4 times lower than these measured values, and k_{off} was identical to the lower value, which resulted in a K_D value (0.74 nmol/L) comparable with other literature reports (Goke et al., 1995; Larsen et al., 1997; Satoh et al., 2000) . The internalization half-life was 7 min [$0.693/k_{int}$], longer than the reported 2-3 min. The discrepancy could be due to the difference between in vivo and in vitro experiments. According to the authors, parts of the receptors continuously recycle back to the cell surface with a half-life of 15 min, without involvement of newly synthesized protein in a significant manner. This process was also handled in the model by using a fixed total receptor concentration (R_{tot}) without a production and degradation process. However, the fraction of recycled GLP-1R was not considered in the current model. The average expression level of the receptors was 14.8 pmol/L/g [5.206 nmol/L/350 g] tissue assuming receptors were evenly distributed throughout the tissues. Goke et al (Goke et al., 1995) reported the binding sites of exendin-4 on the posterior lobe of rat pituitary as 7.8 pmol/L per gram tissue, similar to our estimates especially considering that other tissues (e.g. islets, intestine) may have higher GLP-1R density (Korner et al., 2007).

DMD Fast Forward. Published on February 15, 2012 as DOI: 10.1124/dmd.111.042291
This article has not been copyedited and formatted. The final version may differ from this version.

Different values of K_D for exendin-4 in animals and man have been reported depending on whether a single class or two binding sites were assumed and the cell lines tested. Our estimated human K_D (1.38 nM) was higher than the reported value of 0.82 nM for GLP-1 binding to human pituitary membranes (Satoh et al., 2000). The rat and human GLP-1R exhibit 95% amino acid homology and are 90% identical (Doyle and Egan, 2007), and the K_D values in rats is 53% of values in man. The K_D in monkeys was 0.01% of the other two species, and close to the lower K_D of exendin-4 binding to the rat posterior lobe (Goke et al., 1995). Nevertheless, k_{on} and k_{off} in monkeys and humans are not precisely estimated.

Pharmacodynamics

The PD component of the model reflects the stimulation of insulin secretion by exendin-4. Exendin-4 has to distribute to pancreas and bind to GLP-1R to stimulate insulin release. However, pancreatic GLP-1R is mostly expressed on the surface of the beta cells facing the endothelium (Tornehave et al., 2008), and distribution would be quite fast and therefore a biophase between plasma and pancreas is unnecessary.

One can argue that exendin-4 stimulates insulin secretion by binding to pancreatic GLP-1R and then initiating receptor-mediated signaling pathways. However, in the final PK/PD model, the plasma concentration (*C*), rather than drug-receptor complex (*RC*) was found to work better as the driving force for exendin-4 insulintropic effects. Mathematically, if the effect is driven by *C* (Eq. 7), the transduction between receptor binding and effect is assumed as linear. If the effect is initiated by *RC* (Eq. 8), the transduction between receptor binding and the effect is implied as nonlinear.

Direct evidence supporting Eq. 7 over Eq. 8 came from our observations in Goto-Kakizaki rats (Gao and Jusko, 2011). After an iv bolus of exendin-4, insulin peaked before the maximum concentrations of *RC*. Moreover, since pancreatic GLP-1R are mostly expressed on the surface of the beta cells (Tornehave et al., 2008), exendin-4 can bind to the receptor quite fast and directly stimulate insulin release. Furthermore, binding in other tissues besides pancreas might account for a large portion of drug-receptor complexes.

The basic structure of the PD model represents the feedback mechanism between glucose and insulin. This model utilizes the most simplistic mechanism and functions adequately in various situations. In general, the final estimated parameters controlling glucose and insulin regulation (Table 4) are in accordance with literature values (Jin and Jusko, 2009).

The likely mechanism of action of exendin-4 was integrated into the feedback model using S_d as shown in Eq. 7. The stimulation of exendin-4 on insulin secretion is glucose dependent (Doyle and Egan, 2007). Only when glucose concentrations are higher than a certain threshold is the insulintropic effect evident. This phenomenon was also observed in the rat study: glucose and insulin concentrations did not change during the first 30 min of exendin-4 infusion. This dependency was modeled as the difference of glucose over basal concentrations. When glucose is not higher than basal values, the effect is shut off. The dose-response relationship of exendin-4 both in vitro (Parkes et al., 2001) and in vivo was reported as a bell-shaped curve. Consistently in the initial PD analysis, S_{Glu} increased with dose until 300 pmol/kg/hr and then dropped to a lower value at 3000 pmol/kg/hr. The exact reason for this bell-shaped dose-response

relationship is not clear, but the Adair function adequately captured the relationship between S_{Glu} and plasma concentrations at 30 min (Figure 6A). Later on, the Adair function was directly incorporated into the feedback model to form the PK/PD model. According to the simulations (Figure 8), maximum insulin secretion with this experimental design would be reached at an infusion rate of 120 pmol/kg/min.

Since the Adair function was originally proposed to characterize multiple binding sites on a single receptor, there might be a possibility that a second exendin-4 molecule can bind to the exendin-4- GLP-1R complex, probably when the complex is recycled back to the cell surface. It may be feasible to express the pancreatic GLP-1R as some portion of the total receptor pool and the insulintropic effect proportional to 1:1 drug-receptor complex. To be more mechanistic, the 1:1 complex can be internalized, or dissociated to free receptor with the first dissociation rate constant (k_1), or interact with another exendin-4 molecule with the second dissociation rate constant (k_2).

Other mathematical functions might also describe the bell-shaped dose response relationship, such as a hypothetical antagonist effect generated by exendin-4. But, physiologically, this is not detected in rats, and mathematically, more parameters in the model would lead to over-parameterization. Therefore, the simple Adair function is reasonable for modeling the insulintropic effects of exendin-4.

In conclusion, a mechanistic TMDD PK/PD model was developed that provides quantitative insights into the in vivo PK properties of exendin-4 in various species and the in vivo PD properties in healthy rats. Plasma clearance and volume of distribution followed simple allometric scaling principles across species. The integrated PK/PD model was exemplified using data from healthy rats and well described glucose and

DMD Fast Forward. Published on February 15, 2012 as DOI: 10.1124/dmd.111.042291
This article has not been copyedited and formatted. The final version may differ from this version.

insulin response profiles. This model may prove useful in future animal and clinical studies of exendin-4 and other GLP-1 derivatives.

ACKNOWLEDGMENTS

We are grateful to Brenda Circincione for reviewing this manuscript. Rat and human data were provided by Amylin Pharmaceuticals, Inc.

AUTHORSHIP CONTRIBUTIONS

Participated in research design: Gao and Jusko.

Conducted experiments: Gao.

Contributed new reagents or analytic tools: Not Applicable.

Performed data analysis: Gao.

Wrote or contributed to the writing of the manuscript: Gao and Jusko.

DMD Fast Forward. Published on February 15, 2012 as DOI: 10.1124/dmd.111.042291
This article has not been copyedited and formatted. The final version may differ from this version.

References

Adair GS (1923) On the Donnan Equilibrium and the Equation of Gibbs. *Science* **58:**13.

Ai G, Chen Z, Shan C, Che J, Hou Y and Cheng Y (2008) Single- and multiple-dose pharmacokinetics of exendin-4 in rhesus monkeys. *Int J Pharm* **353:**56-64.

Altaian PL and Dittmer DS (1974) Renal Function Test: Vertebrates. *In Biology Data Book, 2nd ed*. **3:**562-572. Federation of Amer. Society for Exp. Biol., Bethesda, MD.

Copley K, McCowen K, Hiles R, Nielsen LL, Young A and Parkes DG (2006) Investigation of exenatide elimination and its in vivo and in vitro degradation. *Curr Drug Metab* **7:**367-374.

Cvetkovic RS and Plosker GL (2007) Exenatide: a review of its use in patients with type 2 diabetes mellitus (as an adjunct to metformin and/or a sulfonylurea). *Drugs* **67:**935-954.

Degn KB, Brock B, Juhl CB, Djurhuus CB, Grubert J, Kim D, Han J, Taylor K, Fineman M and Schmitz O (2004) Effect of intravenous infusion of exenatide (synthetic exendin-4) on glucose-dependent insulin secretion and counterregulation during hypoglycemia. *Diabetes* **53:**2397-2403.

Doyle ME and Egan JM (2007) Mechanisms of action of glucagon-like peptide 1 in the pancreas. *Pharmacol Ther* **113:**546-593.

Gao W and Jusko WJ (2011) Pharmacokinetic and pharmacodynamic modeling of exendin-4 in type 2 diabetic Goto-Kakizaki rats. *J Pharmacol Exp Ther* **336:**881-890.

Gedulin BR, Smith PA, Jodka CM, Chen K, Bhavsar S, Nielsen LL, Parkes DG and Young AA (2008) Pharmacokinetics and pharmacodynamics of exenatide following alternate routes of administration. *Int J Pharm* **356:**231-238.

Goke R, Fehmann HC, Linn T, Schmidt H, Krause M, Eng J and Goke B (1993) Exendin-4 is a high potency agonist and truncated exendin-(9-39)-amide an antagonist at the glucagon-like peptide 1-(7-36)-amide receptor of insulin-secreting beta-cells. *J Biol Chem* **268:**19650-19655.

Goke R, Larsen PJ, Mikkelsen JD and Sheikh SP (1995) Identification of specific binding sites for glucagon-like peptide-1 on the posterior lobe of the rat pituitary. *Neuroendocrinology* **62:**130-134.

Jin JY and Jusko WJ (2009) Pharmacodynamics of glucose regulation by methylprednisolone. II. normal rats. *Biopharm Drug Dispos* **30:**35-48.

Kagan L, Abraham AK, Harrold JM and Mager DE (2011) Interspecies scaling of receptor-mediated pharmacokinetics and pharmacodynamics of type I interferons. *Pharm Res* **27:**920-932.

Kolterman OG, Kim DD, Shen L, Ruggles JA, Nielsen LL, Fineman MS and Baron AD (2005) Pharmacokinetics, pharmacodynamics, and safety of exenatide in patients with type 2 diabetes mellitus. *Am J Health Syst Pharm* **62:**173-181.

Korner M, Stockli M, Waser B and Reubi JC (2007) GLP-1 receptor expression in human tumors and human normal tissues: potential for in vivo targeting. *J Nucl Med* **48:**736-743.

Larsen PJ, Tang-Christensen M, Holst JJ and Orskov C (1997) Distribution of glucagon-like peptide-1 and other preproglucagon-derived peptides in the rat hypothalamus and brainstem. *Neuroscience* **77:**257-270.

Mager DE, Abernethy DR, Egan JM and Elahi D (2004) Exendin-4 pharmacodynamics: insights from the hyperglycemic clamp technique. *J Pharmacol Exp Ther* **311:**830-835.

Mager DE and Jusko WJ (2001) General pharmacokinetic model for drugs exhibiting target-mediated drug disposition. *J Pharmacokinet Pharmacodyn* **28:**507-532.

Parkes D, Jodka, C., Smith, P., Nayak, S., Rinehart, L., Gingerich, R., Chen, K. and Young, A. (2001) Pharmacokinetic actions of exendin-4 in the rat: Comparison with glucagon-like peptide-1. *Drug Development Research* **53:**260-267.

Parkes DG, Pittner R, Jodka C, Smith P and Young A (2001) Insulinotropic actions of exendin-4 and glucagon-like peptide-1 in vivo and in vitro. *Metabolism* **50:**583-589.

Satoh F, Beak SA, Small CJ, Falzon M, Ghatei MA, Bloom SR and Smith DM (2000) Characterization of human and rat glucagon-like peptide-1 receptors in the neurointermediate lobe: lack of coupling to either stimulation or inhibition of adenylyl cyclase. *Endocrinology* **141:**1301-1309.

Tornehave D, Kristensen P, Romer J, Knudsen LB and Heller RS (2008) Expression of the GLP-1 receptor in mouse, rat, and human pancreas. *J Histochem Cytochem* **56:**841-851.

Widmann C, Dolci W and Thorens B (1995) Agonist-induced internalization and recycling of the glucagon-like peptide-1 receptor in transfected fibroblasts and in insulinomas. *Biochem J* **310 (Pt 1):**203-214.

Footnotes:

This work was supported by the National Institutes of Health [Grant GM 57980].

The current address for the corresponding author, William J. Jusko is as follows: 565 Hochstetter Hall, Department of Pharmaceutical Sciences, University at Buffalo, State University of New York. Buffalo, New York 14260. Email: wjjusko@buffalo.edu.

The current address for Wei Gao is Clinical Pharmacology, Pfizer, Groton, CT 06340.

LEGENDS FOR FIGURES

Figure 1. Scheme of the target-mediated PK/PD model for exendin-4. Symbols are defined in the text and tables.

Figure 2. Exendin-4 concentration versus time profiles following single iv and sc doses of 0.5, 5, 50 nmol and continuous iv infusion at doses of 0.5, 5, 50 nmol/hr in rats. Symbols are mean drug concentrations with error bars representing standard errors (n= 4-7), and solid lines are fitted profiles.

Figure 3. Exendin-4 concentration versus time profiles following single iv and sc doses of 1, 3, 10 μg/kg in monkeys. Symbols are mean drug concentrations with error bars representing standard errors (n= 3), and solid lines are fitted profiles.

Figure 4. Exendin-4 concentration versus time profiles following single sc doses (upper panel: study A, middle panel: study B) and iv infusion (bottom panel: study C) in humans. Symbols are mean drug concentrations with error bars representing standard errors (n= 7-8), and solid lines are fitted profiles.

Figure 5. Time profiles of glucose (left) and insulin (right) concentrations in rats during saline (A) or drug (B: 3, C: 30, D: 300 and E: 3000 pmol/kg/min) infusions with glucose bolus challenge at 30 min. Symbols are mean concentrations with error bars representing standard errors (n= 4-8), and solid lines are fitted profiles.

Figure 6. Simulated exendin-4 concentration profiles at various infusion rates in the PD study (A) and the relationship between S_{Glu} estimates and exendin-4 concentration at 30 min after the start of drug infusions (B).

Figure 7. The relationship of estimated values of k_a versus dose (A) and selected PK parameters (CL_c (B), V_c (C) and k_{off} (D)) versus body weight in rats, monkeys and man.

Figure 8. Simulated insulin responses (pM) after glucose challenge with various exendin-4 infusion rates according to the PK/PD model.

DMD Fast Forward. Published on February 15, 2012 as DOI: 10.1124/dmd.111.042291
This article has not been copyedited and formatted. The final version may differ from this version.

Table 1. Parameters obtained from NCA analysis of concentration profiles in rats. Parameters λ_1, λ_2, CL, V_{ss} and CL_D were calculated from mean profiles after iv bolus, and $Dose/C_{ss}$ was calculated from mean profiles after continuous iv infusion.

iv bolus						iv infusion	
Dose (nmol)	λ_1 (min^{-1})	λ_2 (min^{-1})	*CL* (ml/min)	V_{ss} (ml)	CL_D (ml/min)	*Dose* (nmol/hr)	$Dose/C_{ss}$ (ml/min)
0.5	0.297	0.0363	4.99	44.8	1.08	0.5	7.25
5	0.133	0.0240	3.40	57.3	0.751	5	4.42
50	0.137	0.0174	3.39	68.2	0.818	50	3.17

Table 2. Parameter estimates obtained from the time profiles of exendin-4 in rats with the TMDD model.

Parameter (units)	Definition	Estimate (CV%)
k_{el} (min^{-1})	Elimination rate constant	0.0839 (10)
k_{pt} (min^{-1})	Intercompartmental rate constant	0.0282 (15)
k_{tp} (min^{-1})	Intercompartmental rate constant	0.0213 (5)
V_c (ml)	Central volume of distribution	43.2 (12)
k_{on} ($nmol^{-1}.min^{-1}$)	Second-order binding constant	0.0207 (42)
k_{off} (min^{-1})	First-order dissociation constant	0.0153 (206)
k_{int} (min^{-1})	Internalization rate constant	0.0966 (38)
k_a1 (min^{-1})	Absorption rate constant at 0.5 nmol	0.00820 (9)
k_a2 (min^{-1})	Absorption rate constant at 5 nmol	0.00579 (11)
k_a3 (min^{-1})	Absorption constant at 50 nmol	0.00273 (11)
F	Bioavailability	1 (fixed)
R_{tot} (nmol/L)	Total receptor concentration	5.21 (5)

Table 3. Parameter estimates of exendin-4 in monkeys and man based on the TMDD model.

Parameter (units)	Definition	Monkeys (CV%)	Humans (CV%)
k_{el} (min^{-1})	Elimination rate constant	0.0346 (10)	0.013 (198)
k_{pt} (min^{-1})	Intercompartmental rate constant	0.0143 (17)	0.0685 (262)
k_{tp} (min^{-1})	Intercompartmental rate constant	0.00593 (17)	0.0846 (168)
V_c (ml/kg)	Central volume of distribution	69.3 (12)	111 (168)
k_{on} ($pmol^{-1}.min^{-1}$)	Second-order binding constant	0.272 (607)	0.000411 (351)
k_{off} (min^{-1})	First-order dissociation constant	0.0326 (2990)	0.566 (399)
k_{int} (min^{-1})	Internalization rate constant	0.00211 (179)	0.00342 (587)
k_a (min^{-1})	Absorption rate constant for various dose groups	0.0244 -0.0142 (10-14)	0.00550 – 0.0148 (14-17)
F	Bioavailability	0.688 (8)	1 (fixed)
R_{tot} (pmol/L)	Total receptor concentration	60.6 (33)	1240 (fixed)

Table 4. Parameter estimates obtained from the glucose and insulin profiles after IV glucose challenge during saline or exendin-4 infusions in rats using the TMDD PK/PD model.

Parameter (units)	Definition	Estimate (CV%)
k_{outG} (1/min)	Glucose elimination rate constant	0.046 (9)
k_{outI} (1/min)	Insulin elimination rate constant	0.483 (50)
S_{INS} (1/nMol)	Stimulation factor of insulin on glucose disposal	0.157 (46)
S_{GLU} (1/mMol)	Stimulation factor of glucose on insulin secretion	0.0684 (20)
V_g (L/kg)	Glucose apparent volume of distribution	0.208 (5)
S_{max}	Maximum response factor	4.67 (30)
k_1 (nMol)	First receptor binding constant	0.826 (71)
k_2 (1/nMol)	Second receptor binding constant	0.0153 (69)

Figure 1.

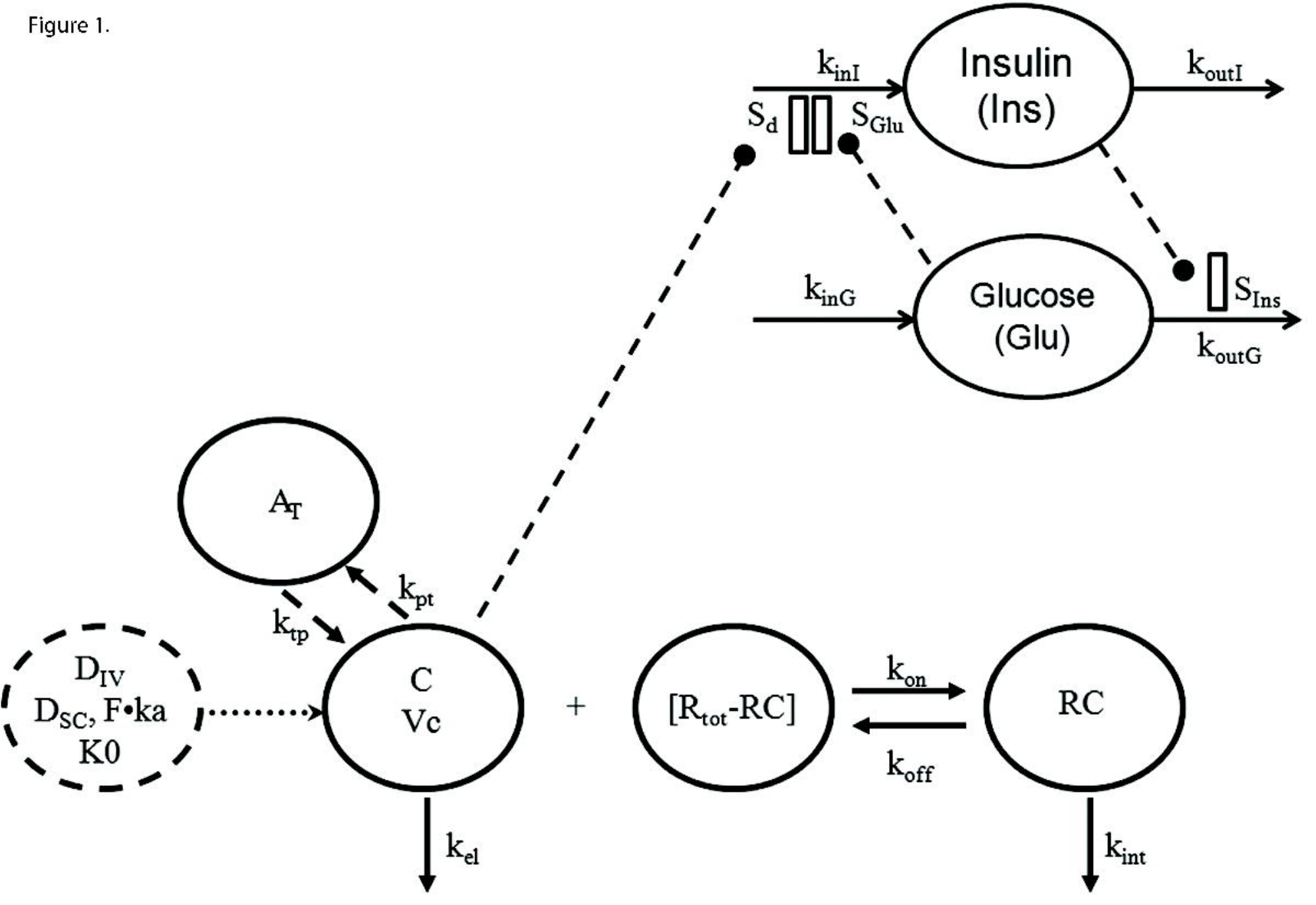
k_{inI}
Insulin
(Ins)
k_{outI}
S_d
S_{Glu}
k_{inG}
Glucose
(Glu)
S_{Ins}
k_{outG}
A_T
k_{pt}
k_{tp}
D_{IV}
D_{SC}, F•ka
K0
C
Vc
+
$[R_{tot}$-RC]
k_{on}
k_{off}
RC
k_{el}
k_{int}

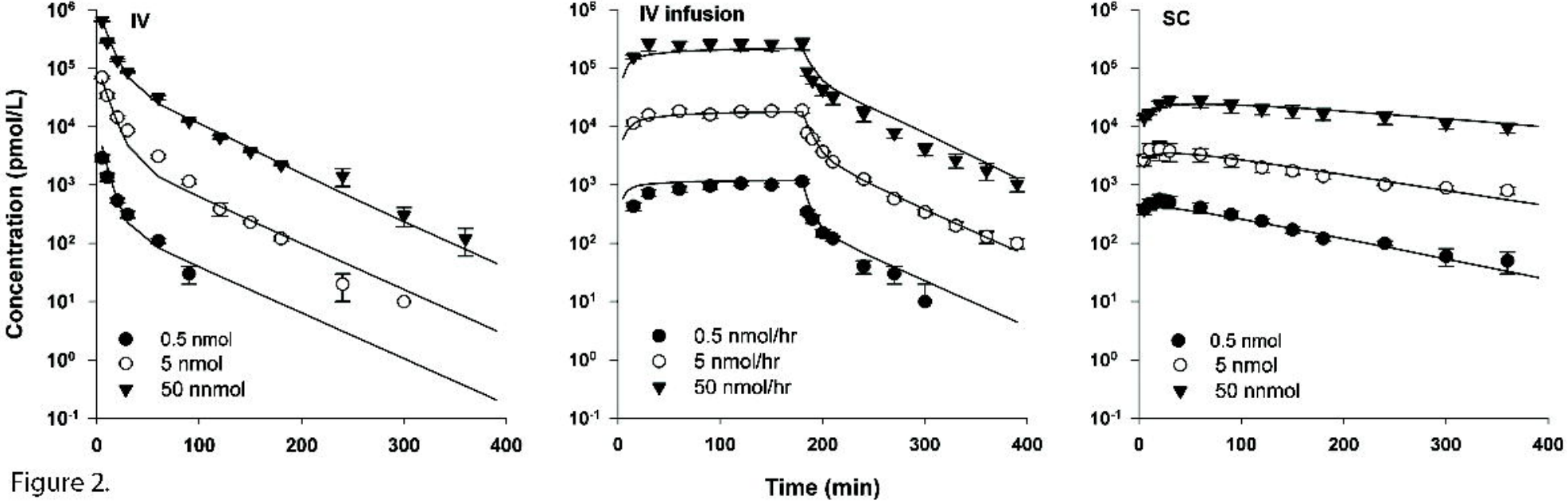
IV
IV infusion
SC
Concentration (pmol/L)
Time (min)
0.5 nmol
5 nmol
50 nnmol
0.5 nmol/hr
5 nmol/hr
50 nmol/hr
0
100
200
300
400

Figure 2.

Figure 3.

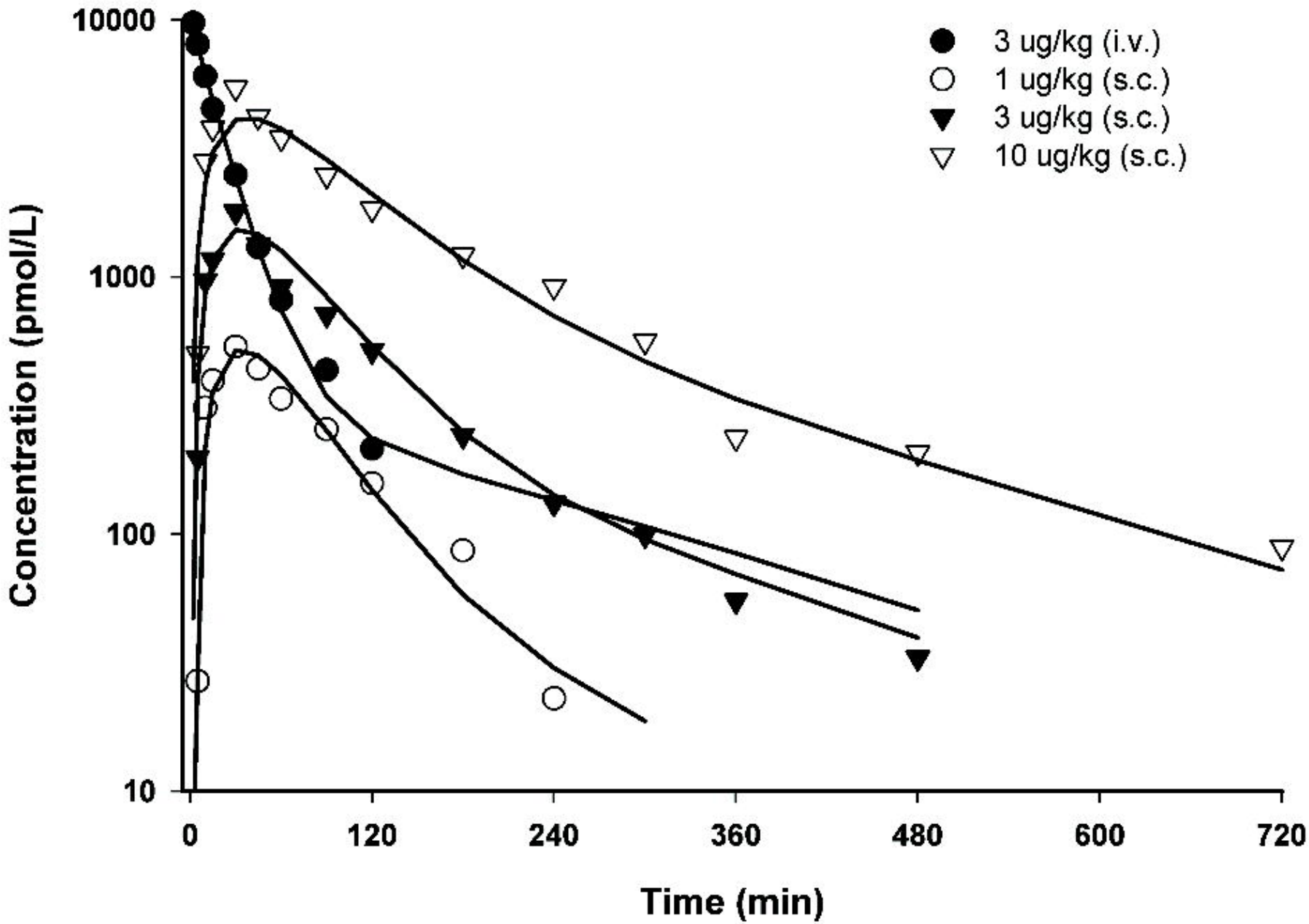
10000
1000
100
10
Concentration (pmol/L)
0
120
240
360
480
600
720
Time (min)
3 ug/kg (i.v.)
1 ug/kg (s.c.)
3 ug/kg (s.c.)
10 ug/kg (s.c.)

Figure 4.

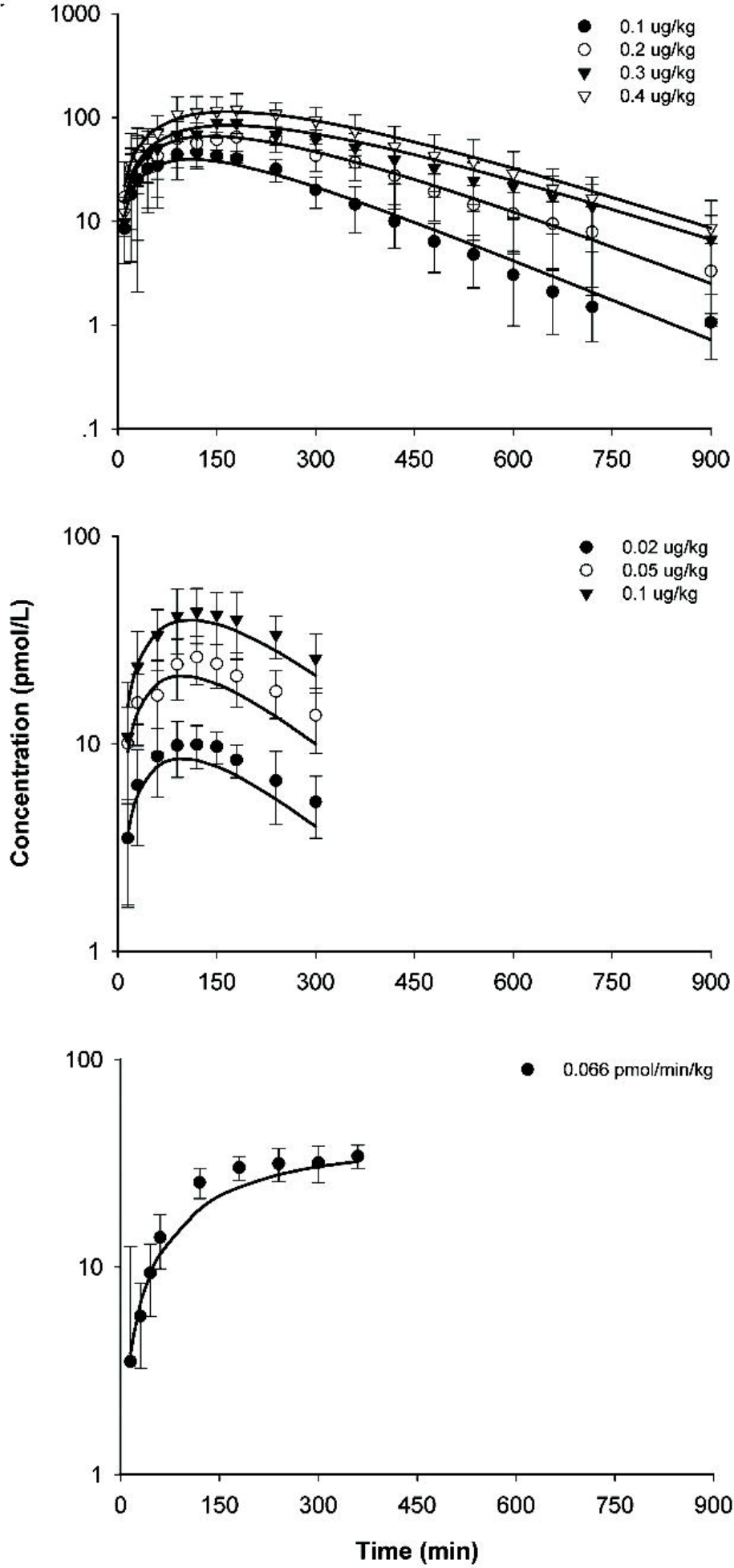
1000
100
10
1
.1
0
150
300
450
600
750
900
0.1 ug/kg
0.2 ug/kg
0.3 ug/kg
0.4 ug/kg
100
10
1
0.02 ug/kg
0.05 ug/kg
0.1 ug/kg
Concentration (pmol/L)
100
10
1
0.066 pmol/min/kg
Time (min)

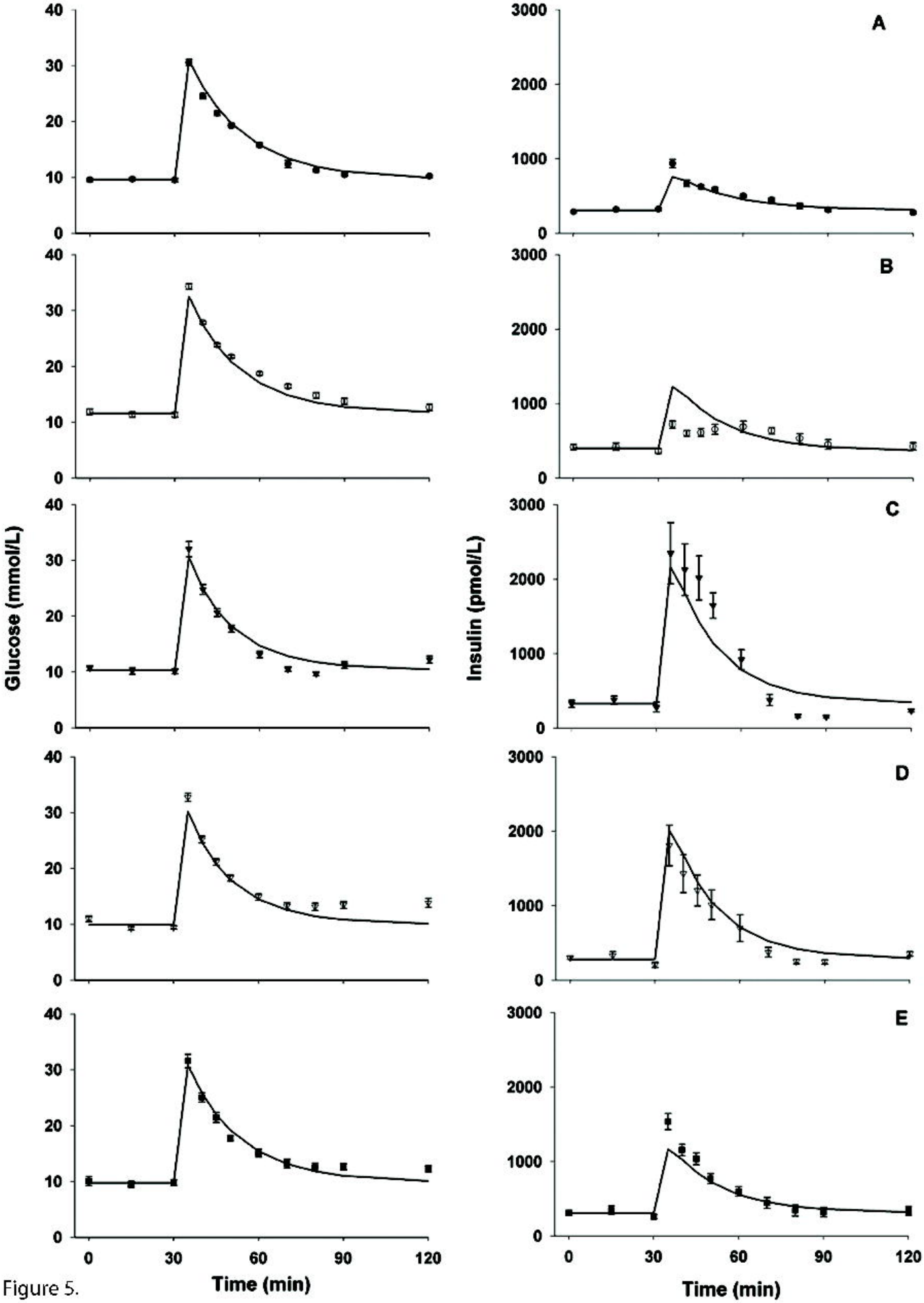
A
B
C
D
E
Glucose (mmol/L)
Insulin (pmol/L)
Time (min)
Time (min)
0
10
20
30
40
1000
2000
3000
0
30
60
90
120

Figure 5.

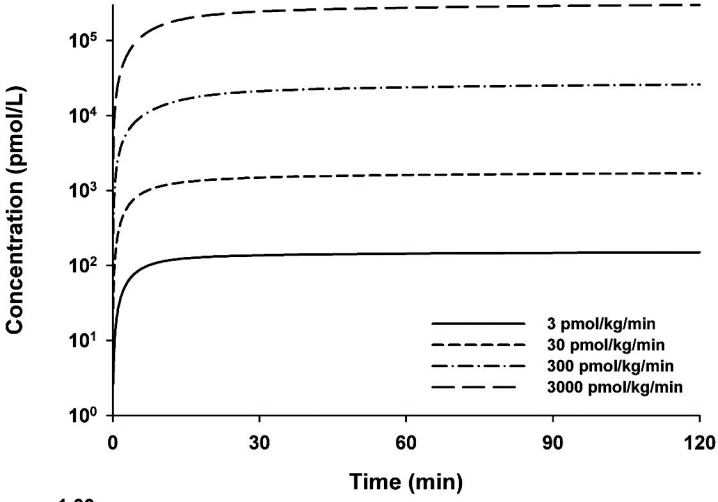
Concentration (pmol/L)
10^5
10^4
10^3
10^2
10^1
10^0
0
30
60
90
120
Time (min)
3 pmol/kg/min
30 pmol/kg/min
300 pmol/kg/min
3000 pmol/kg/min

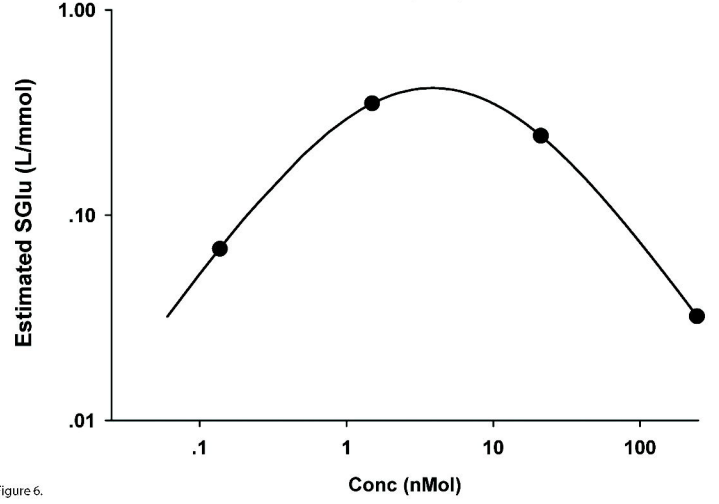
Estimated SGlu (L/mmol)
1.00
.10
.01
.1
1
10
100
Conc (nMol)

Figure 6.

Figure 7

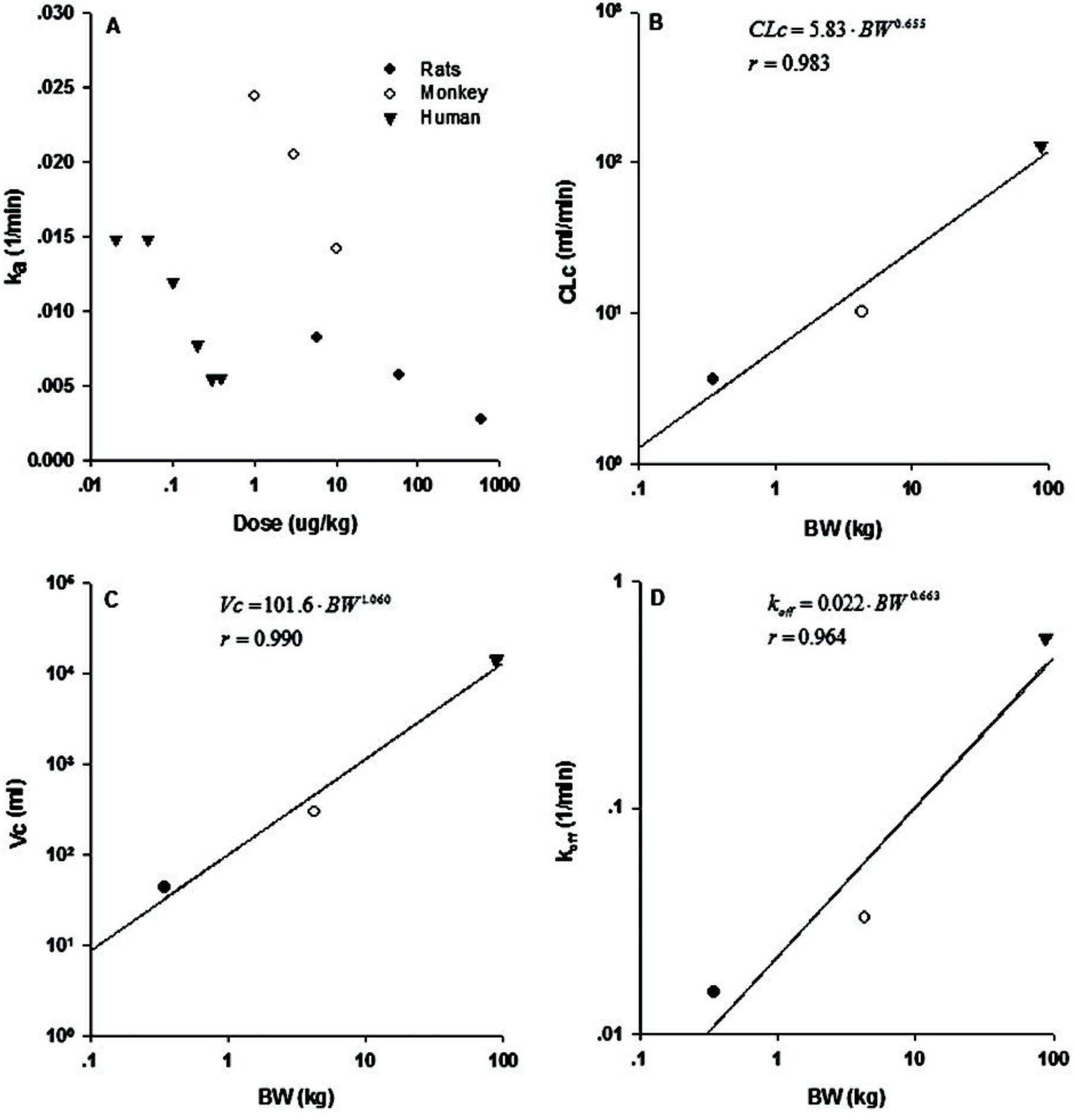
A
Rats
Monkey
Human
k_a (1/min)
Dose (ug/kg)
B
$CLc = 5.83 \cdot BW^{0.655}$
$r = 0.983$
CLc (ml/min)
BW (kg)
C
$Vc = 101.6 \cdot BW^{1.060}$
$r = 0.990$
Vc (ml)
BW (kg)
D
$k_{off} = 0.022 \cdot BW^{0.663}$
$r = 0.964$
k_{off} (1/min)
BW (kg)

Figure 8

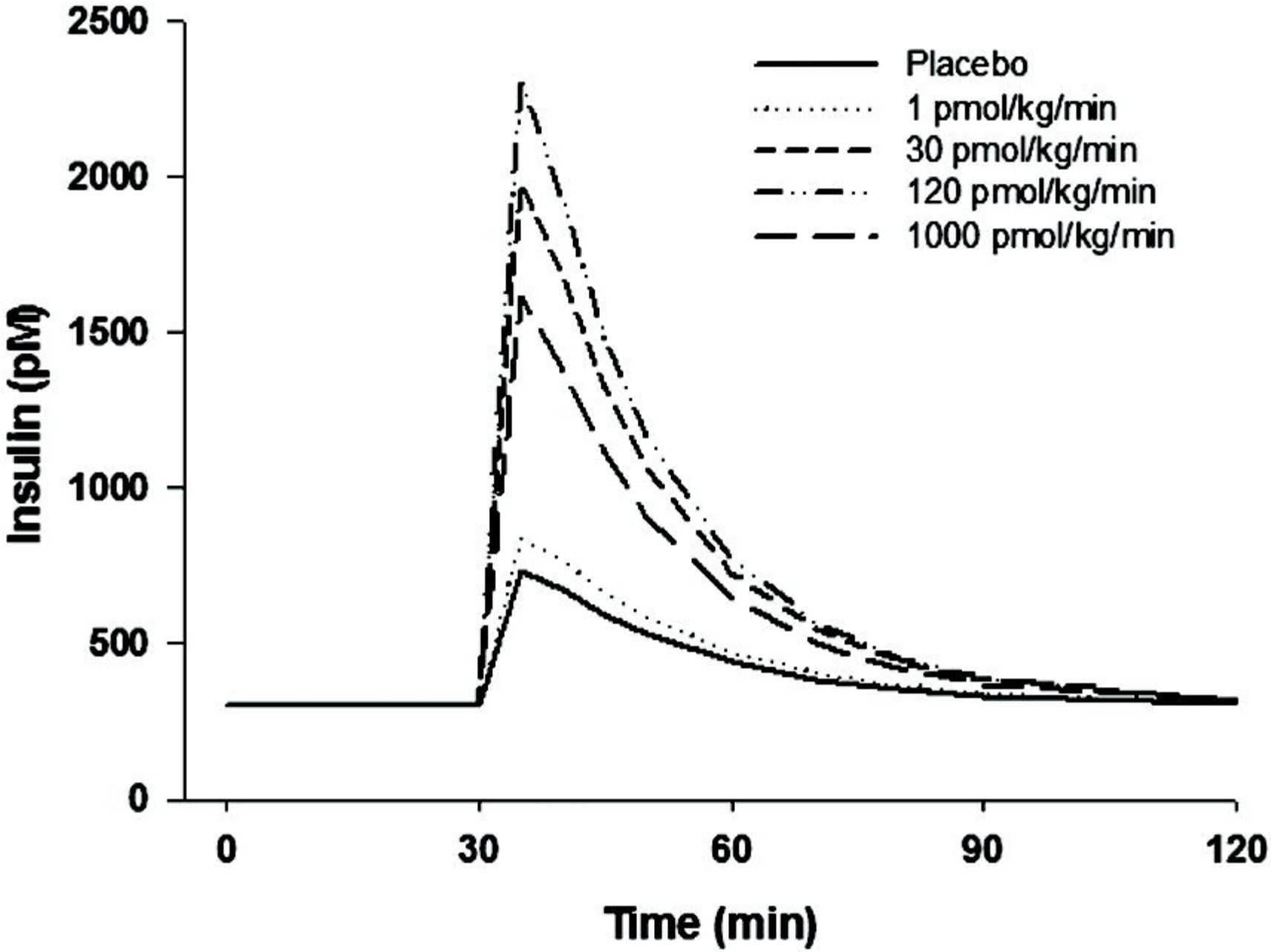
2500
2000
1500
1000
500
0
Insulin (pM)
0
30
60
90
120
Time (min)
Placebo
1 pmol/kg/min
30 pmol/kg/min
120 pmol/kg/min
1000 pmol/kg/min